I- Reionization (8)
II- First Stars (4)
III- High-z QSOs (4)
IV- Ly-α emitters LAE (3)
V- Deep surveys (2)

Poster Session

Far Away: Light in the young Universe beyond redshift three

Françoise Combes, Paris Observatory

I- Reionization

S. Baek
D. Crociani
S. Gallerani
G. Harker
V. Jelic
U. Maio
R. Thomas
J. Van Bethlehem

Baek, DiMatteo, Semelin, Combes, Revaz

21cm signal from the EoR, with full Ly-α transfer

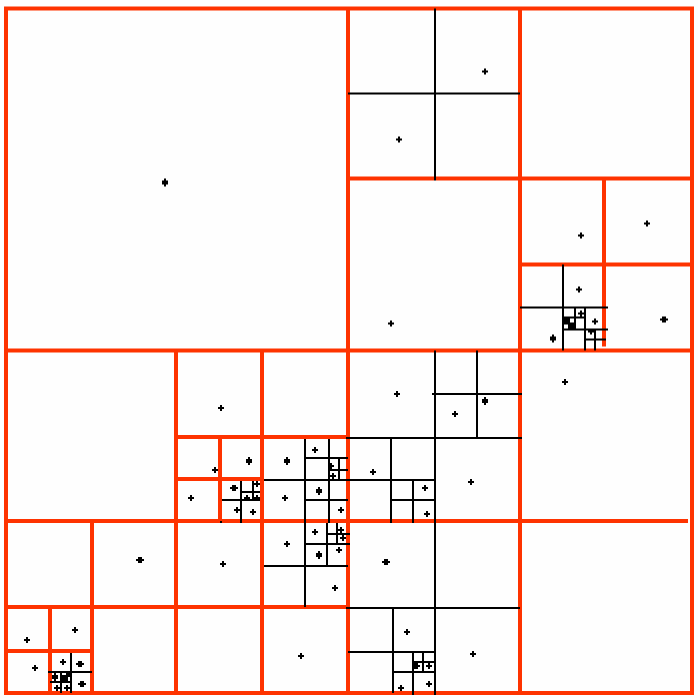

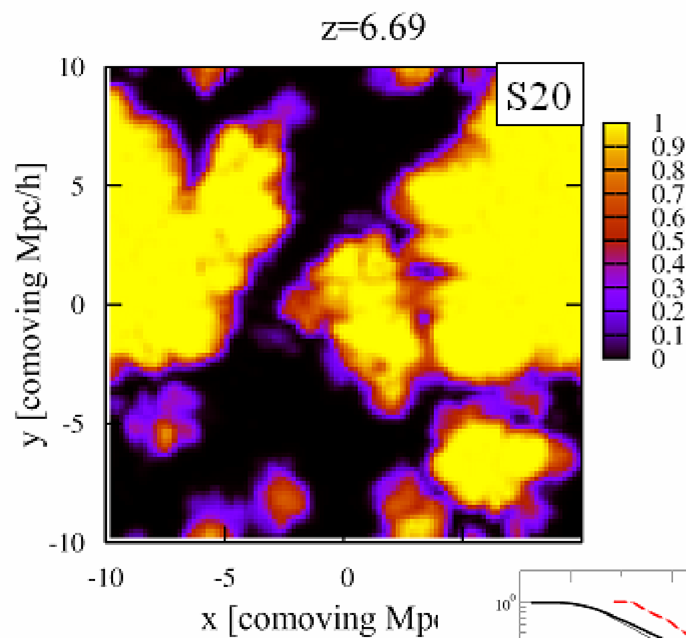

Ionising fraction

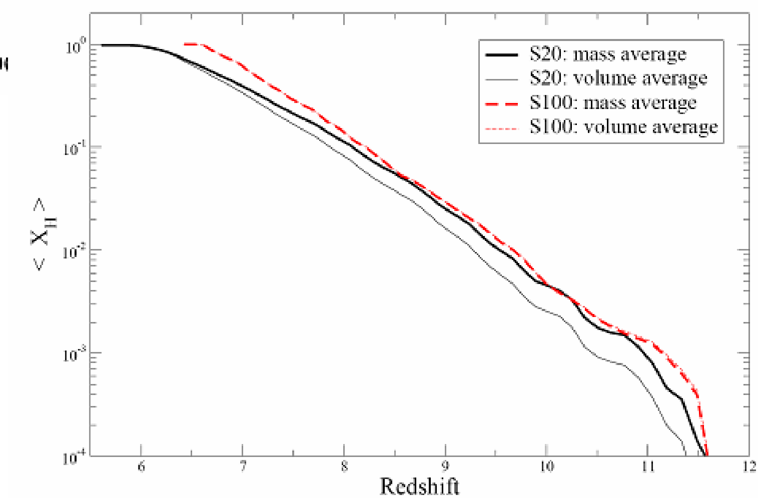

(a) Mass weighted and volume weighted averaged ionization fraction.

LICORICE: adaptive grid, dynamics with TreeSPH, and orange grid for RT Continuum UV and Ly-α line

Crociani, Moscardini, Viel, Bartelmann & Meneghetti

EoR in alternative cosmological scenarios

1) Quintessence cosmology: with a z-dependent dark energy component, either Peebles & Ratra (2003) (RP) or Brax & Martin (2000) (SUGRA);

2) Non-Gaussian universe: both scale-independent (local) and scale dependent (equilateral) non-Gaussianities are considered (Loverde et al. 2007).

With quintessence: 1) enhanced formation of larger HII regions at the same z and **2)** higher typical bubbles radius neglecting IGM recombination (Fig 1a). This effect is smoothed by the IGM recombination (Fig 1b) .

In a non-Gaussian universe: 1) enhanced ionised fraction at high z and **2)** 10% effects of the non-Gaussianity on the IGM optical depth (Fig. 2).

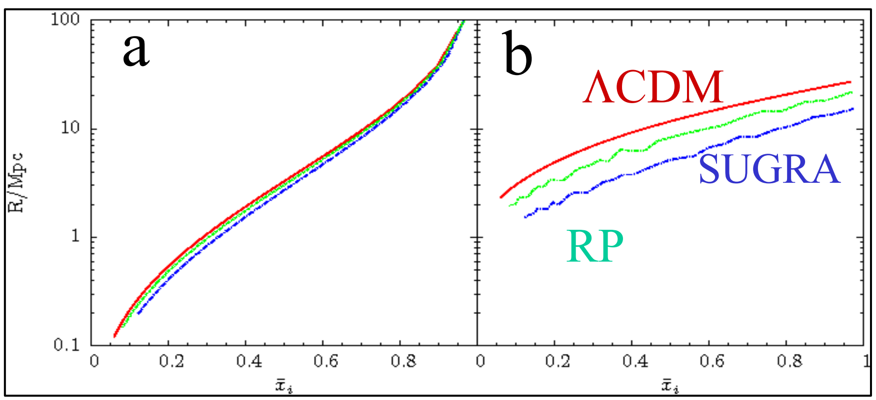

Fig 1. Bubble radius without (panel a) and with (panel b) IGM recombination

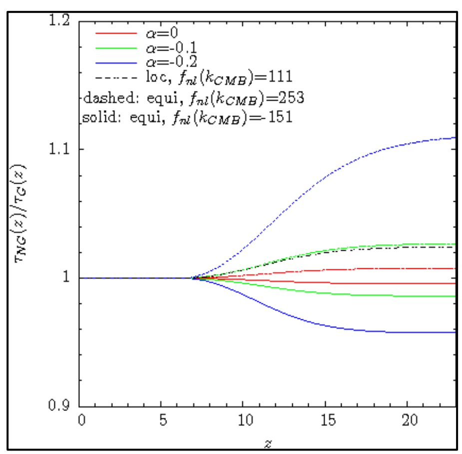

Fig. 2 IGM optical depth ratios for the non-Gaussian and the Gaussian cases, assuming both local (black) and equilateral (colour lines) shapes, with different scale-dependence α.

Gallerani, Ferrara, Choudhury, Dayal, Fan & Salvaterra

The imprints of reionization on the young Universe

Two reionization scenarios: an Early Reionization Model (**ERM**) in which IGM is reionized at z_{rei}~7, and a Late Reionization Model (**LRM**) in which overlapping occurs at z_{rei}~6.

QSOs, GRBs and LAEs at z~6 to discriminate between the two

SAM to simulate Ly-α forest in QSO/GRB

Results are consistent with a high ionization, and then with ERM

Compatible with LAE LF (z=4.5-6.6)

➔Extended reionization period between z=11 and 7, as in WMAP5

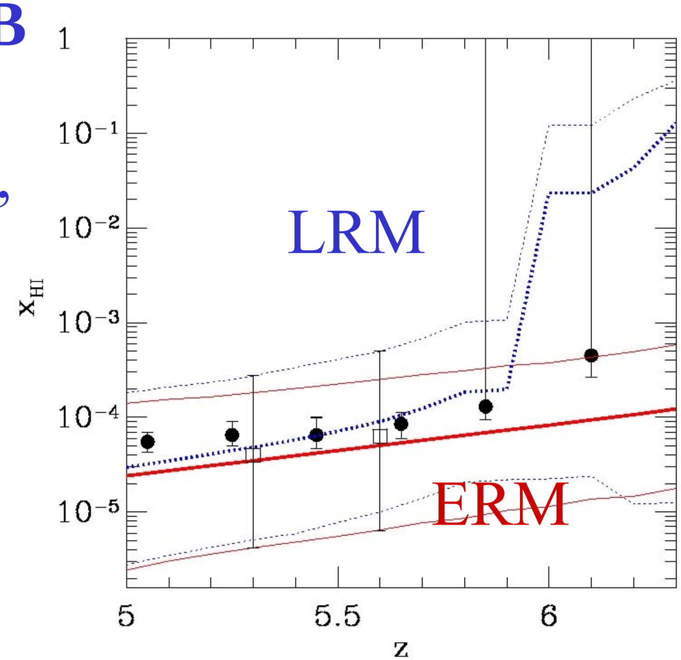

Harker, Zaroubi & LOFAR EoR team

Statistics to extract and analyze the 21cm signal from the EoR

- It will be a challenge to extract the 21cm signal from the EoR.
- This signal is expected to be complex and non-Gaussian.
- First step towards using this structure not only to compare models, but to extract the cosmological signal from realistic foregrounds, instrumental effects and noise in the first place.

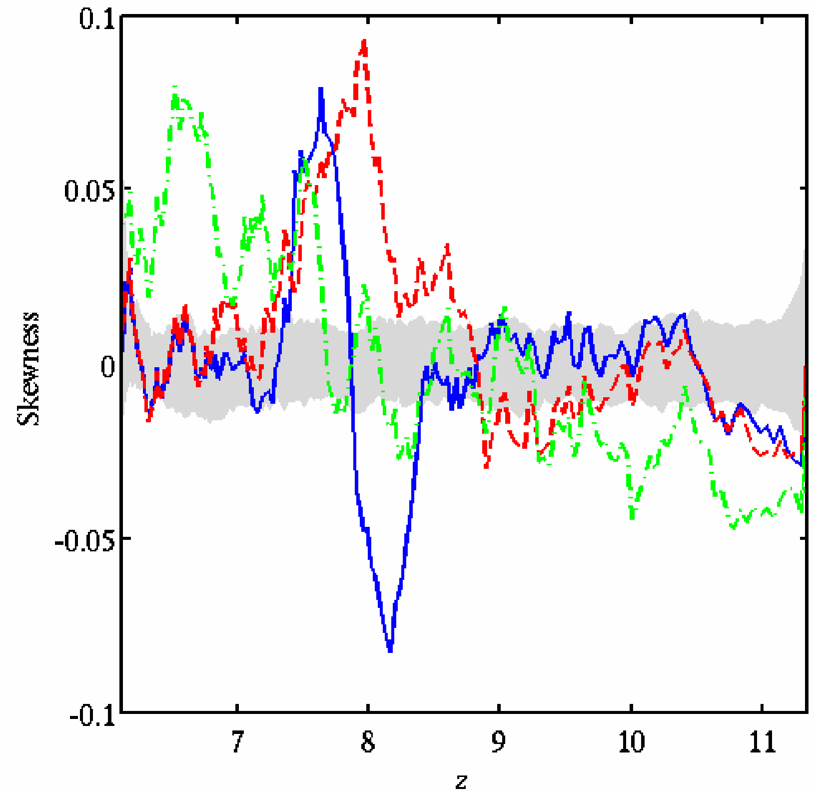

➔ skewness, a route to detection and to discriminate different models

Jelic, Zaroubi, Labropoulos et al
The foreground simulations for the LOFAR-EoR experiment

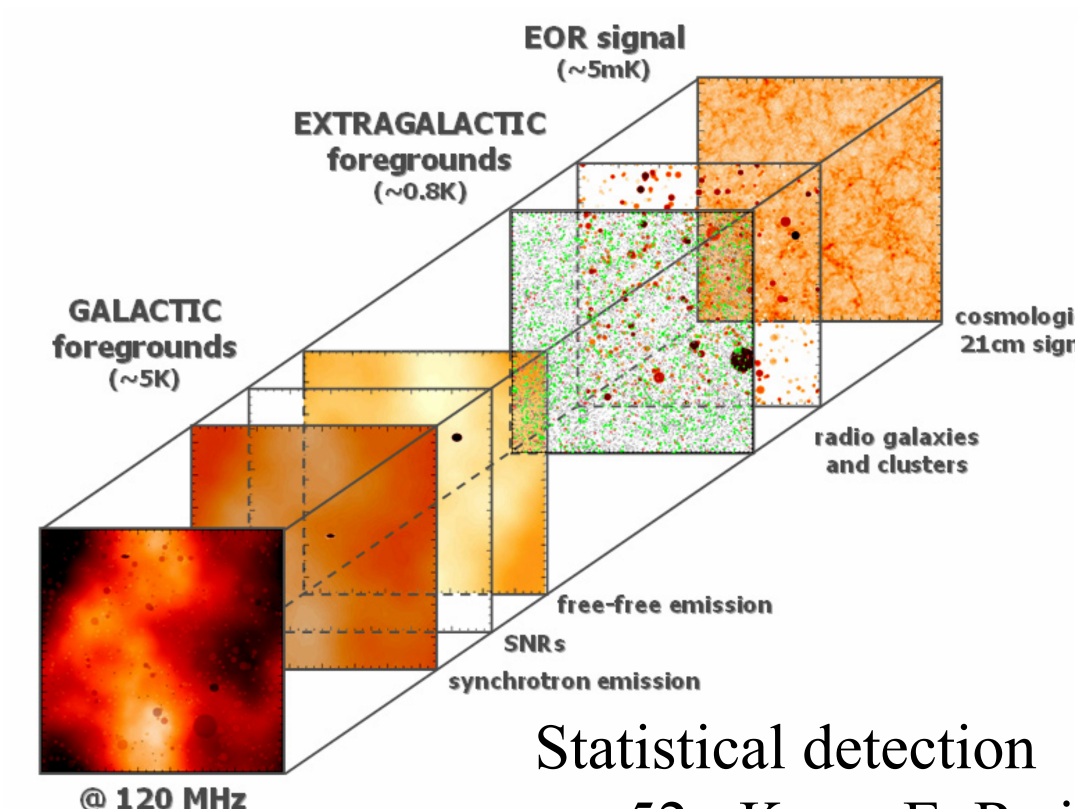

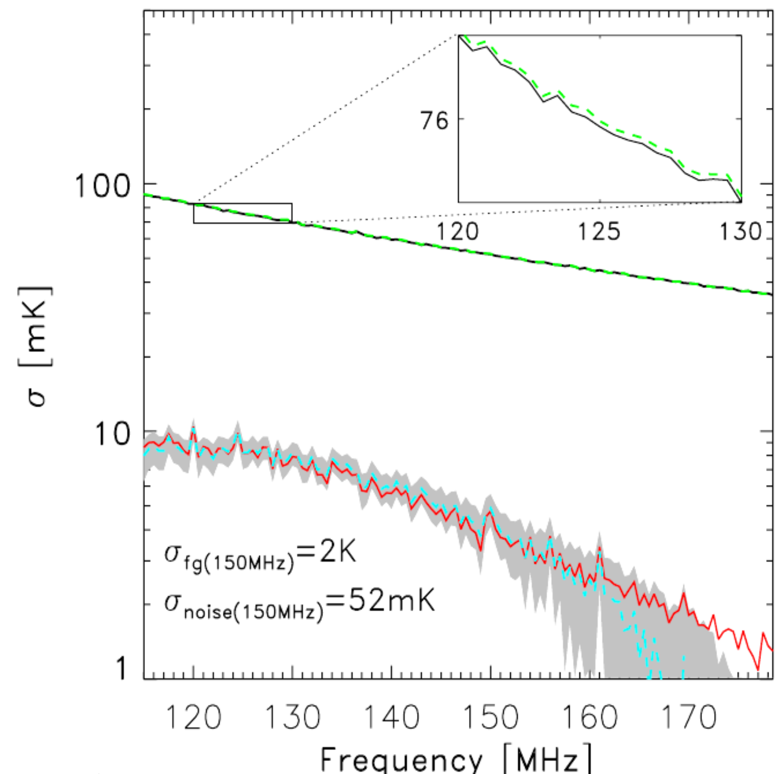

Statistical detection

σ= 52mK —— EoR signal

--- residuals after removing the diffuse foreground

Maio, Ciardi, Dolag, Tornatore & Yoshida

Early molecules, star formation and metal pollution

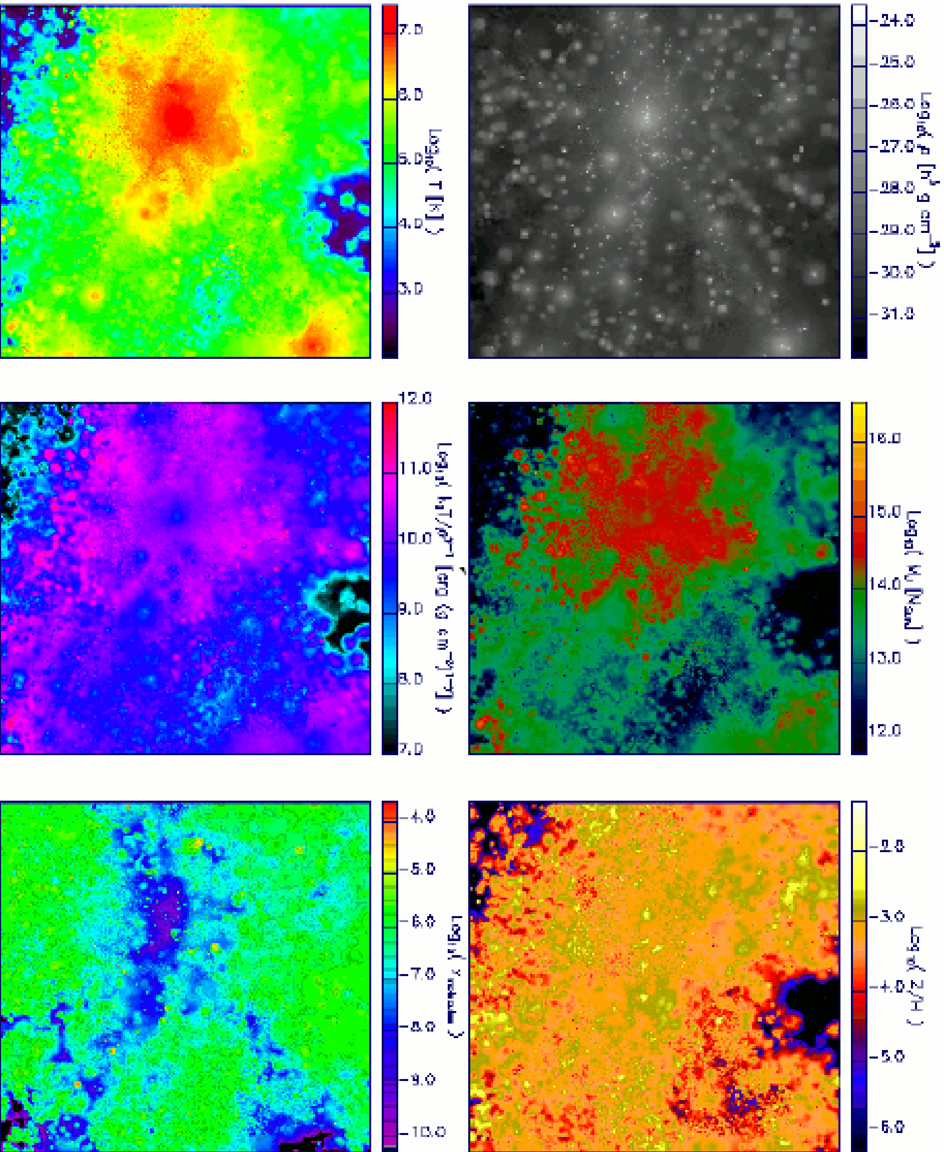

T ρ

S m_J

Mol Metal

➔ Uncorrelation Mol - SF

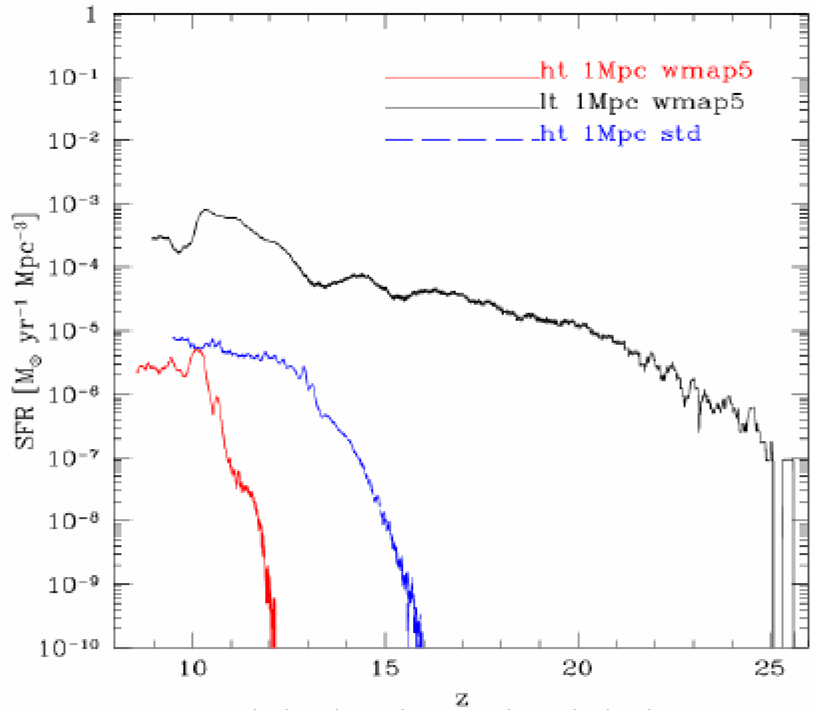

Low or high threshold for SF

Thomas, Zaroubi & Ciardi

21(1+z)cm EoR signal for LOFAR

BEARS: Bubble Expansion Around Radiative Sources

Algorithm using the homogeneity of Universe at z>6
5minutes single processor, instead of 35h CRASH

CRASH

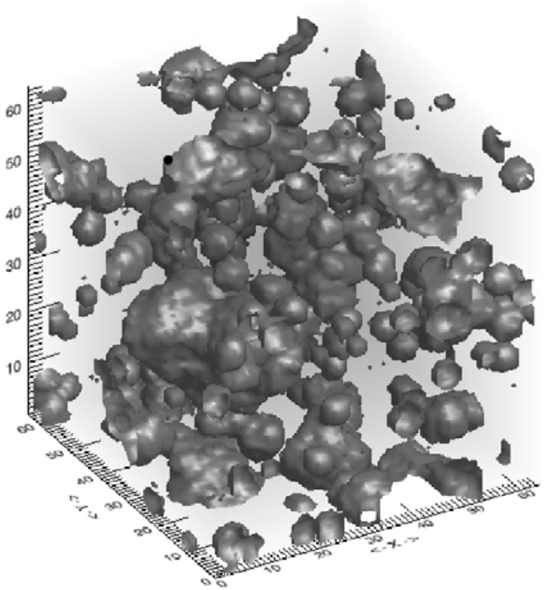

BEARS

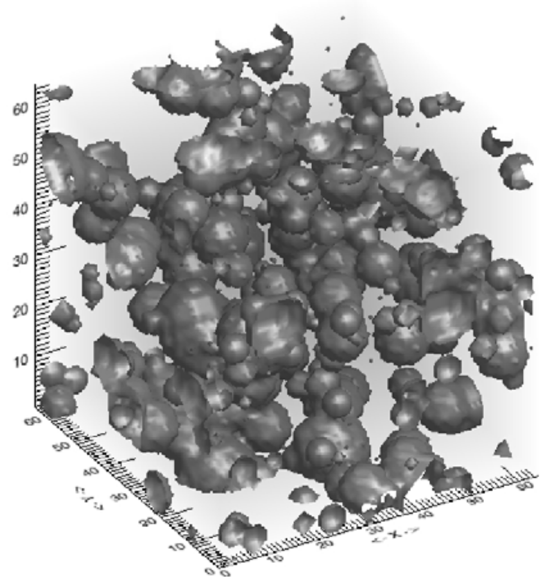

Can allow to vary parameters quickly quasars stars, etc..

Van Bethlehem

Simulating radiative transfer during the EoR using unstructured grids

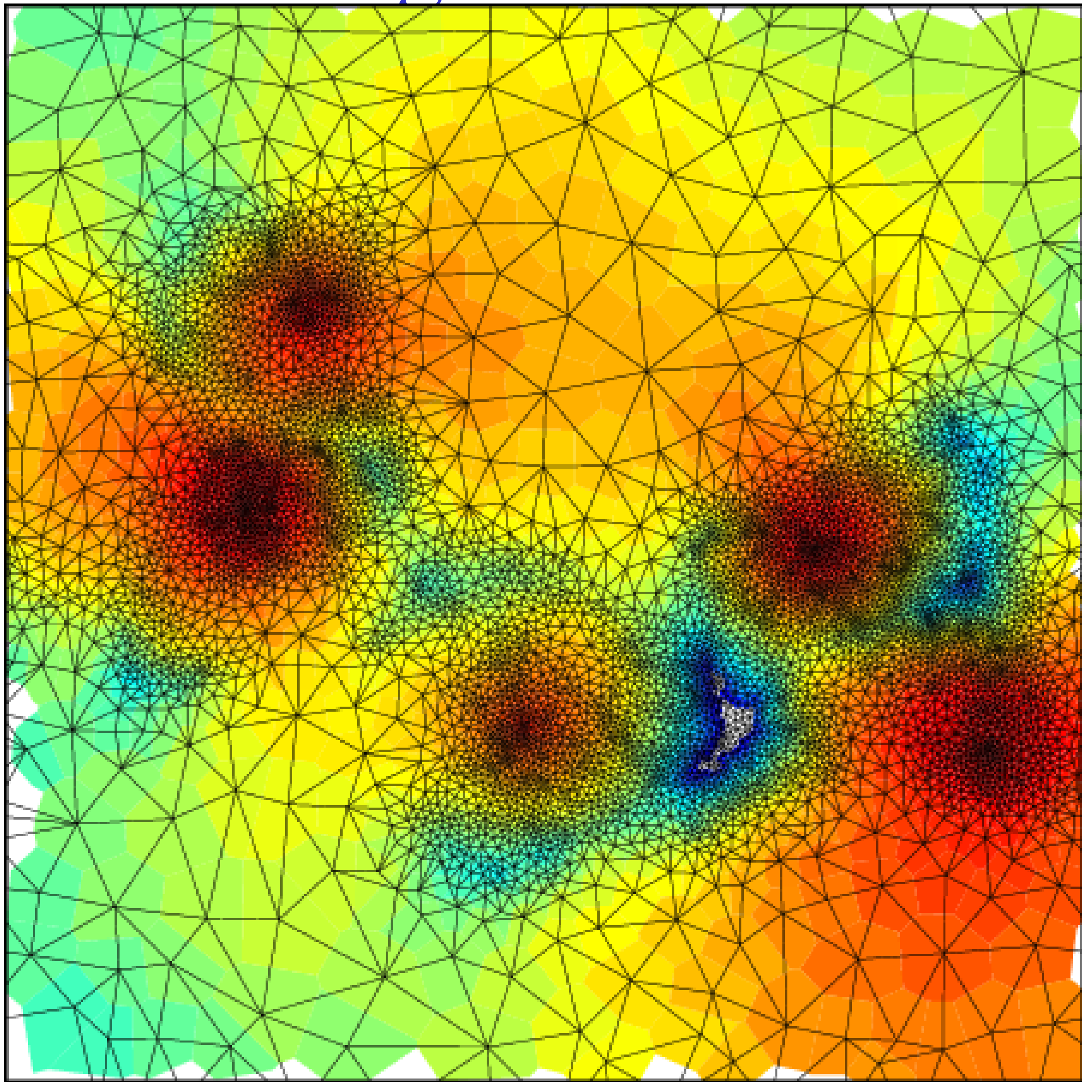

6761 grid points
4 sources in the densest parts
Photons are diffusing
All physics coupled to the grid

Adaptative resolution
Colour= nbr of photons after
26 transport iterations

From dark blue to red (high)

White= no photon yet

II- First Stars

C. Evoli
D. Maurin
A. Raiter
P. Vonlanthen

Evoli, Salvadori & Ferrara

The puzzling origin of the ^{6}Li plateau

^{6}Li abundance followed in a Hierarchical model of galaxy Formation

MPHS Fe/H reproduced

CR spallation formation of ^{6}Li

Contrary to previous claims (Rollinde et al 2006)

➔Large discrepancy

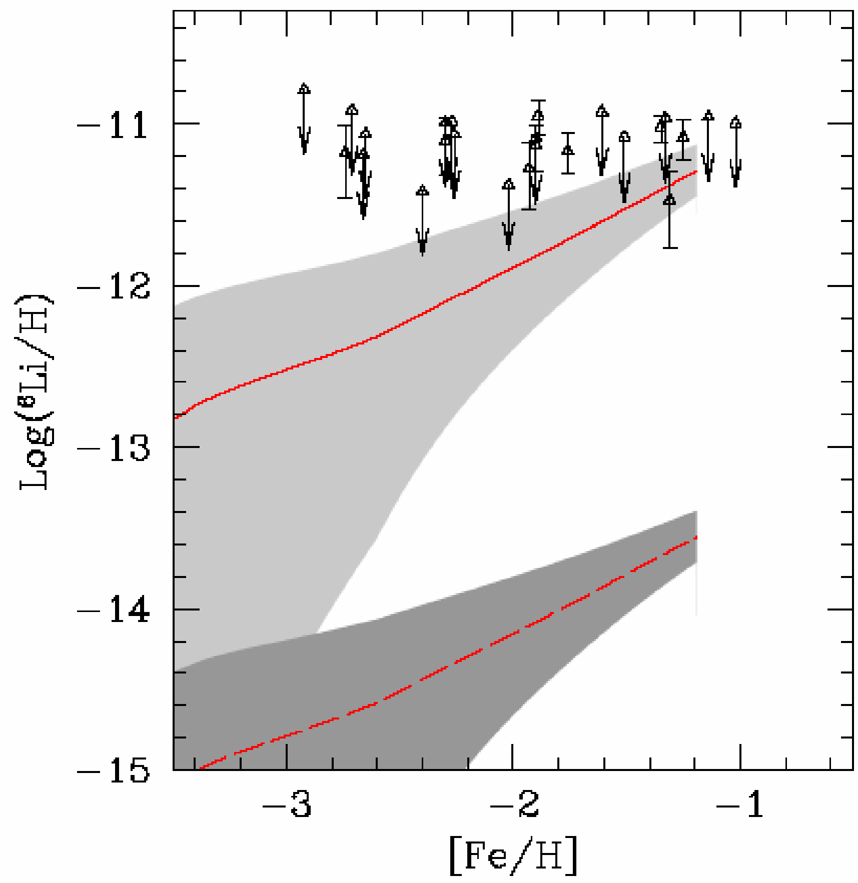

Figure 4. Redshift evolution of ^{6}Li/H vs [Fe/H] for the fiducial model (**dashed line**) and for the maximal model (**solid line**). Shaded areas denote $\pm 1\sigma$ dispersion regions around the mean of the input SFR.

Maurin, Rollinde, Vangioni, Olive & Inoue

Cosmological CR production of Li, Be, B

- ^{6}Li abundance in Pop II stars of the galactic halo has been observed at 1000 times the BBN value.
- Its cosmological production depends on the escape efficiency ε of CCRs from the hierarchical structures at a given z.

➔ε is adjusted to account for the Li data (typically 0.15 for the best scenario (see model 1 in figures) in cosmic hierarchical structure formation (Pop III + Pop II/I stars)

The associated non-thermal (NT) BeB and γ-ray evolutions with z in the intergalactic medium (IGM) is calculated.

- Early cosmic BeB enrichment is coherent with observed abundances in halo stars at z = 3.
- The associated extragalactic γ-ray background is well below existing EGRET data.

Prompt initial enrichm
(PIE)
^{6}Li/H=$10^{-11.2}$

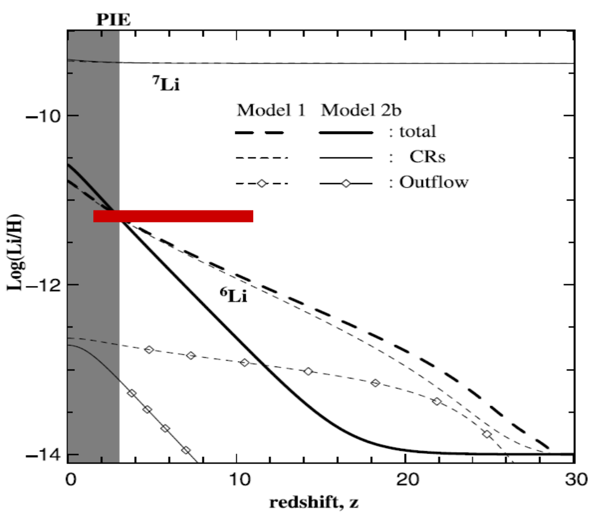

Be/H=10^{-13}
In star G64-1

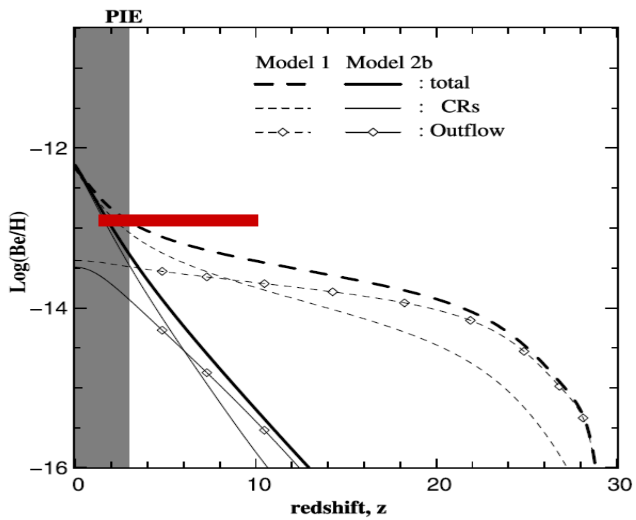

➔ *NT LiBeB nucleosynthesis can be used as a new tracer to constrain early Pop III stars.*

Raiter

Modeling the spectra of the first stars: the nebular geometry effects

Using photoionization models, and theoretical stellar SED

Goal: to find a simple representative structure for further studies

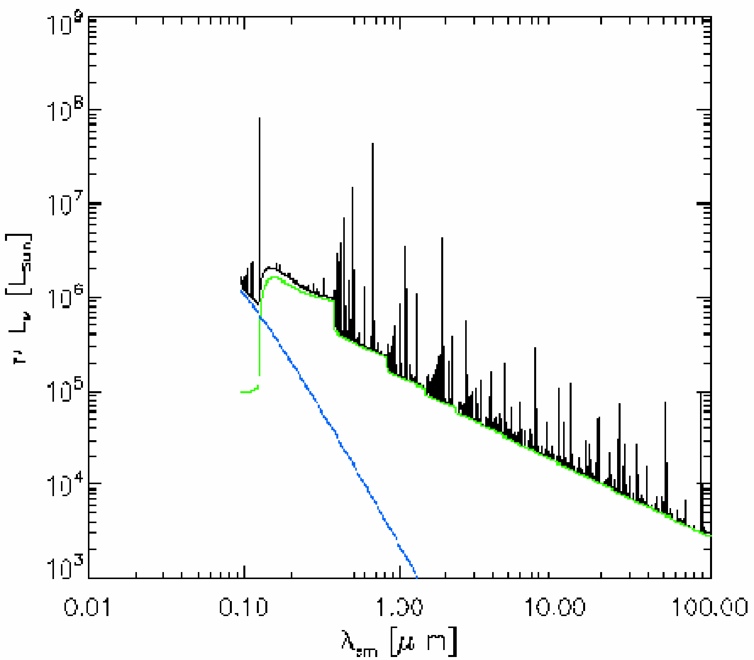

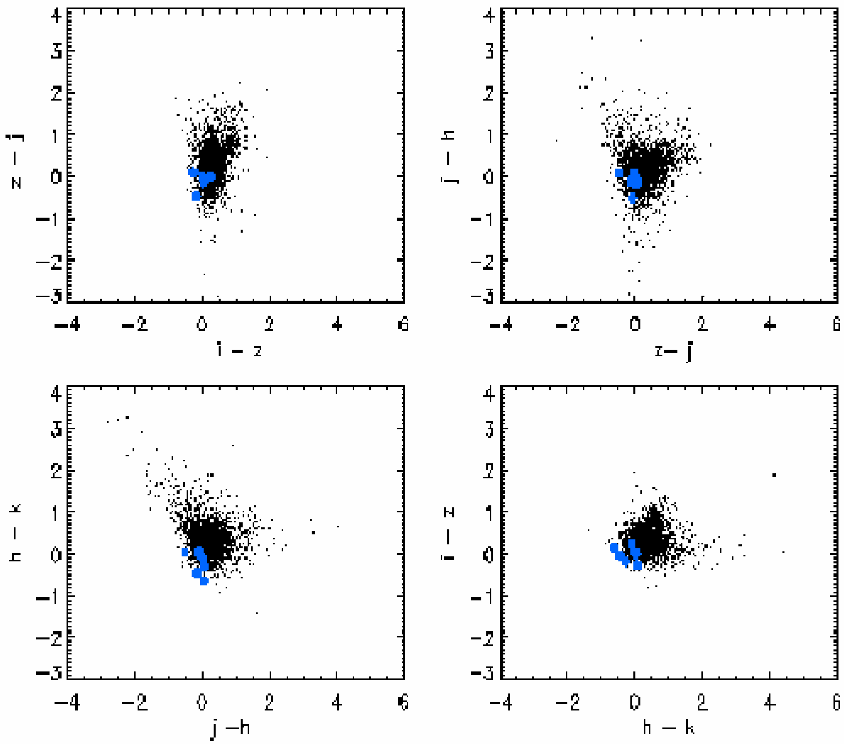

CLOUDY ➔ COLOR-COLOR DIAGRAMS

Vonlanthen & Puy

H_2 and HD cooling in gravitational collapses

Cooling functions of H_2 and HD in the standard model (left) and in a non-homogeneous nucleosynthesis model able to form hea nuclei (right). Right: HD is more abundant than H_2.
Compared in a simple 1D gravitational collapse.

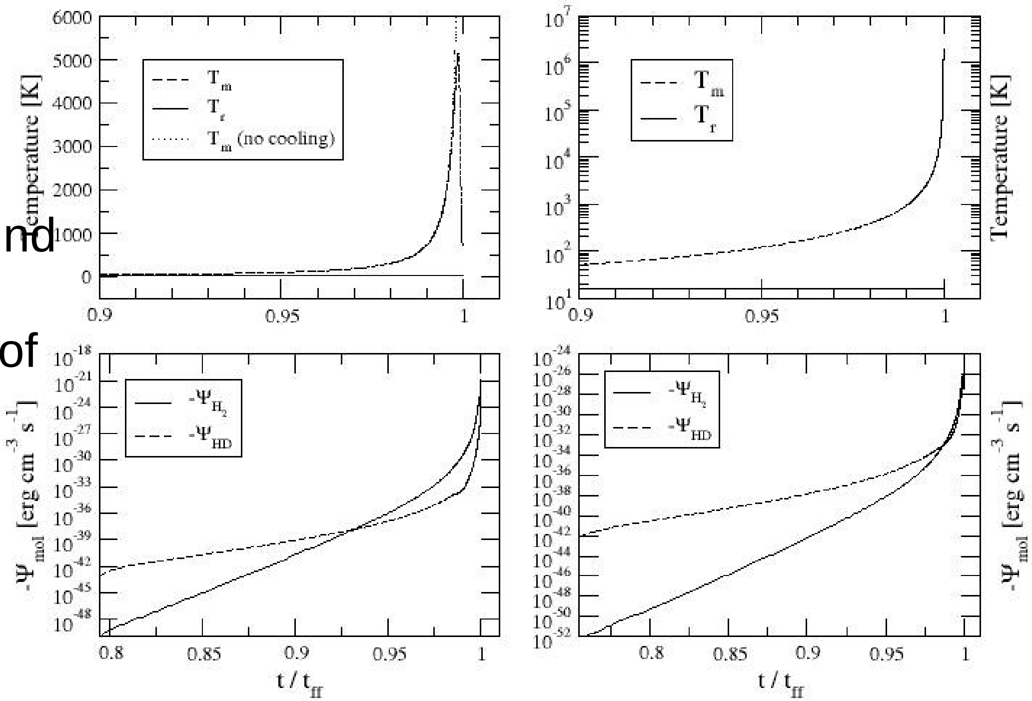

- influence on H and D chemistry, of the non-thermal radiation background produced by the cosmological H recombination (leading to a decrease of H_2 and HD abundances).
- collisions with H, He and H_2, with recent rate coefficients.

➔HD never cools efficiently

III- High-z QSOs

L. Christensen
F. Fontanot
S. Frey
P. Tisserand

Christensen

Quiescent haloes of radio quiet quasars

Results from IFU studies of 17 QSOs at 2.5 < z< 4.5

- **Lyα halos around radio quiet QSOs are likely ubiquitous. (See preliminary study in Christense et al. 2006)**

- **Halo properties:**
  - **narrow emission lines (~500 km/s)**
  - **luminosities log L(Lyα)~ 10^{43} erg/s**
  - **fainter than radio loud quasars' nebulae**

Future investigations:

- **Are halos around radio quiet QSOs systematical fainter than around radio loud QSOs? Or just due to different investigation techniques**

- **Determine presence of inflows/outflows from kinematics and morphologies**

- **Estimate halo masses**

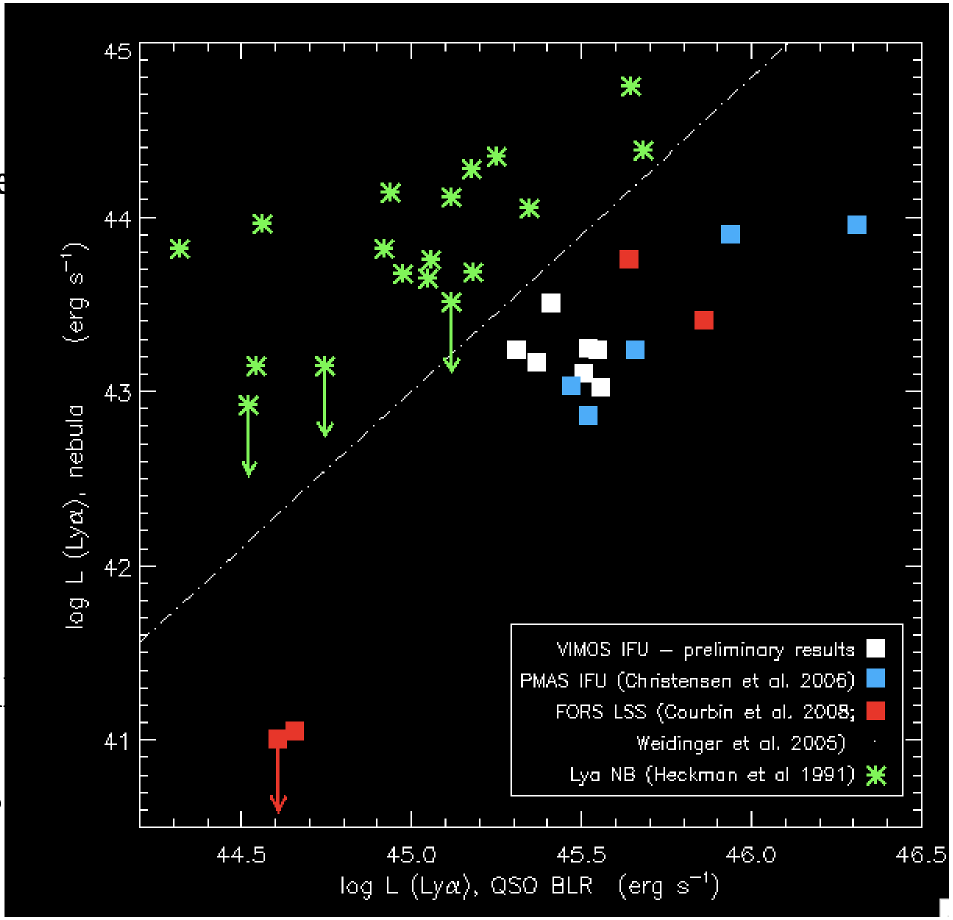

Fontanot, Cristiani, Monaco et al

The LF of QSOs for 3.5 < z < 5.2 GOODS & SDSS

Models based on pure **density evolution** show better agreement with observations than do models based on pure **luminosity evolution**. However a different break magnitude with respect to z~2.1 is required

FAINT END

Models with a steep faint-end (power-law exponent between -1.49 and -1.71) score a higher probability

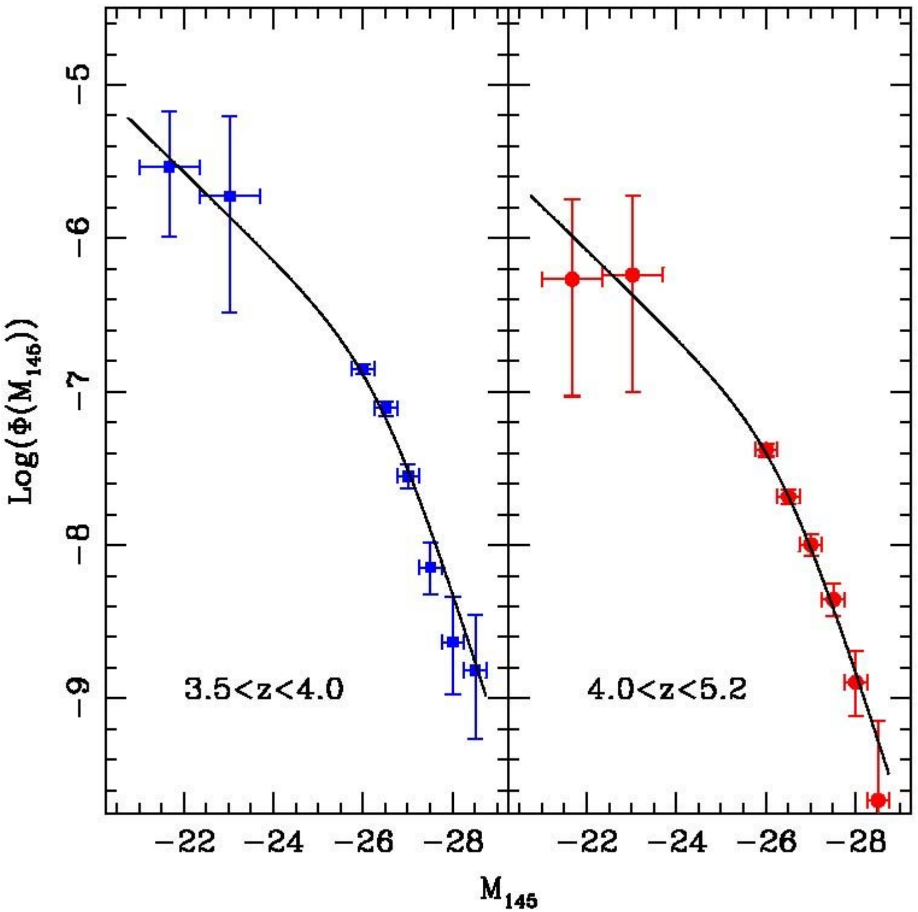

BRIGHT END

No evidence for a flattening of the bright-end with respect to low-z observations

➔ due to the different estimate of the completeness of the SDSS sample

Frey

The 10-100pc scale radio structure of the only radio-loud quasar at z>6

J1427+3312 (*z*=6.12): a working AGN at 0.9 Gyr after the Big Bang

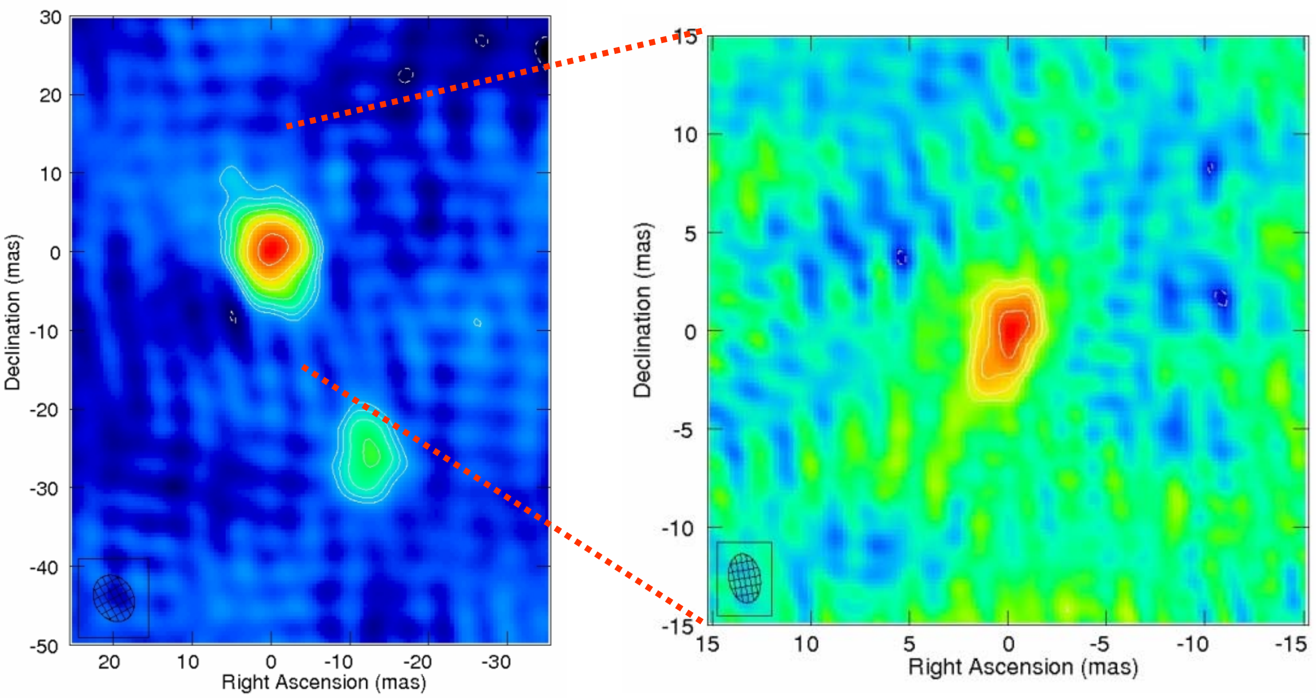

successfully imaged with VLBI at two frequencies on milli-arcsecond scales

double radio stucture: a Compact Symmetric Object?
this + other evidence → maybe a very young (~1000 yr) source

Tisserand, Keller, Schmidt, Bessel & Francis

The SkyMapper and the high-z QSOs

Australian 1.3m telescope, 268 Mega pix, 5.7 deg^2, 6 colors, 6 epochs

1st light Jan 2009, http://www.mso.anu.edu.au/skymapper

All sky 20 000 deg^2, 1 mag deeper than SDSS, 1 billion objects

170 QSO at z>5.8 will be found

(10 times more than SDSS)

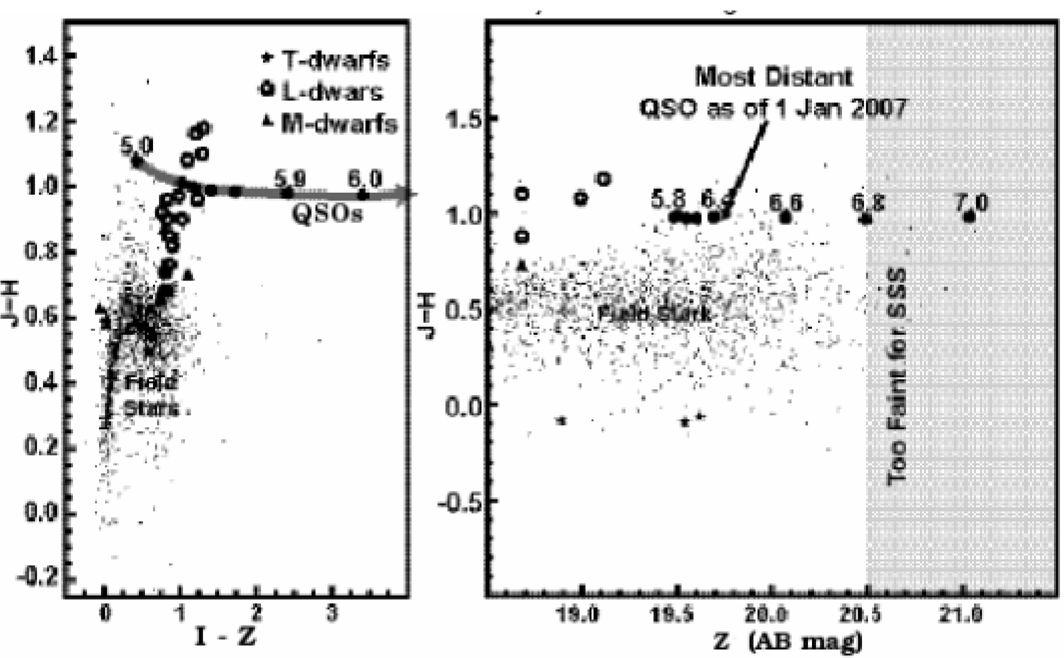

IV- Ly-α emitters LAE

B. Clement
S. Finkelstein
A. Verhamme

Clement, Cuby, Kneib, Hibon, Bouché & Richard

Surveys for LAE beyond z=7, clusters or blank fields

- **Blind search of z ~ 9 Lyman-alpha emitters behind the cluster Abell 1689 (SINFONI)**
- Critical lines scanning
- 20hrs this semester, reduction and analysis in progress
- 20hrs accepted for next semester
- 21 pointings that do not overlap in the source plane except for those targeting Stark et al. candidates (Stark et al 2007; ApJ, 663, 10)

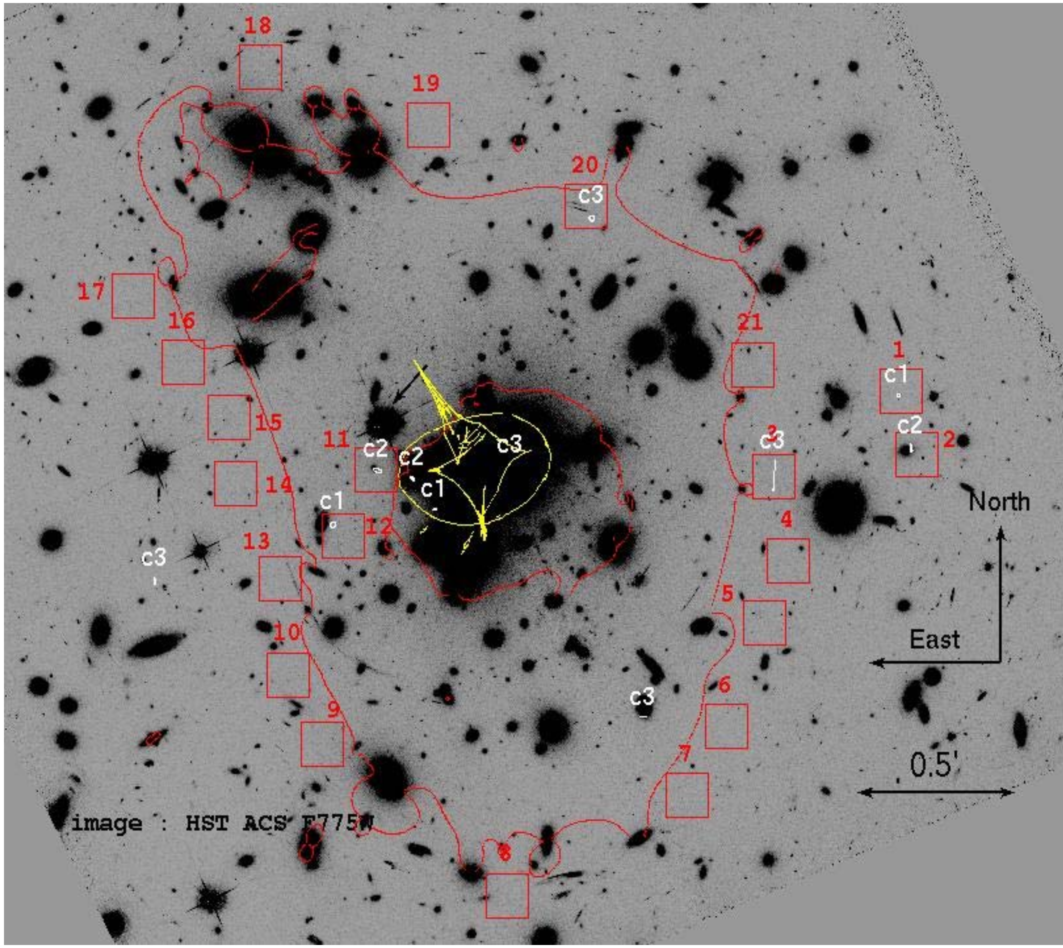

red: critical lines, yellow: caustic lines, c1/c2/c3 : Stark candidates and counter images

Finkelstein, Rhoads, Malhotra, Grogin

Ly-α galaxies:primitive, dusty or evolved?

- All 15 LAEs at z ~ 4.5 contain some amount of dust.
    - A_{1200} = 0.3 - 4.5
- In 2/3 of the sample, the ISM has a clumpy geometry, which results in the dust preferentially attenuating the continuum more than Lyα.
    - Enhances the Lyα equivalent width.
- This allows an old galaxy to be detected in a narrowband survey.

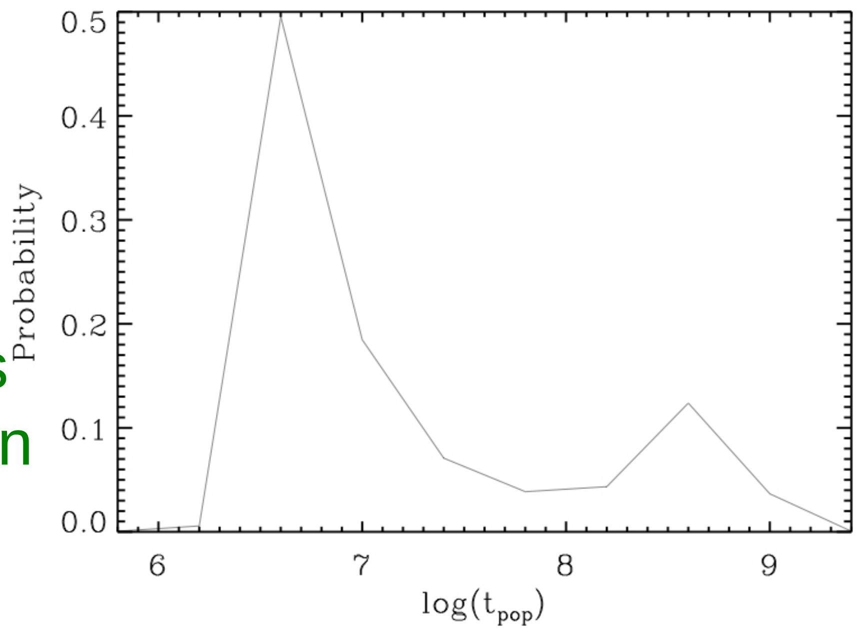

- found a bimodal age distribution for LAEs.
    - Either young or old, but always dusty, thus not primitive.

Verhamme, Schaerer, Atek & Tapken

Constraints on gas and stellar properties of z~3 LBGs from the fitting of Ly-α lines

MCLyα, spherical expansion. **Escape fraction depends on extinction**

All trends in LAE and LBG come from NHI and associated dust

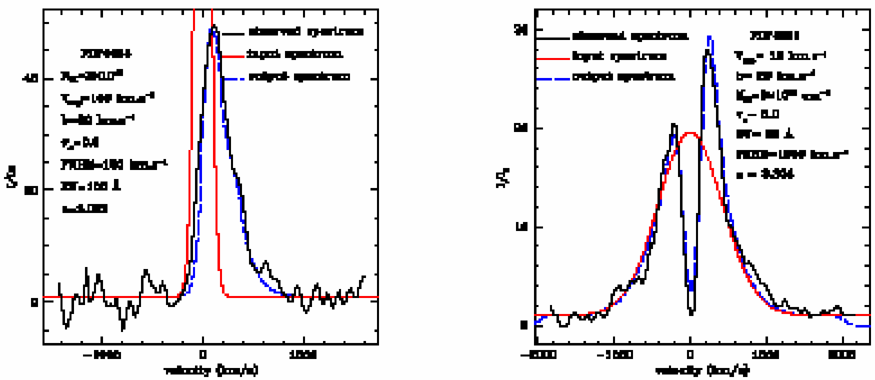

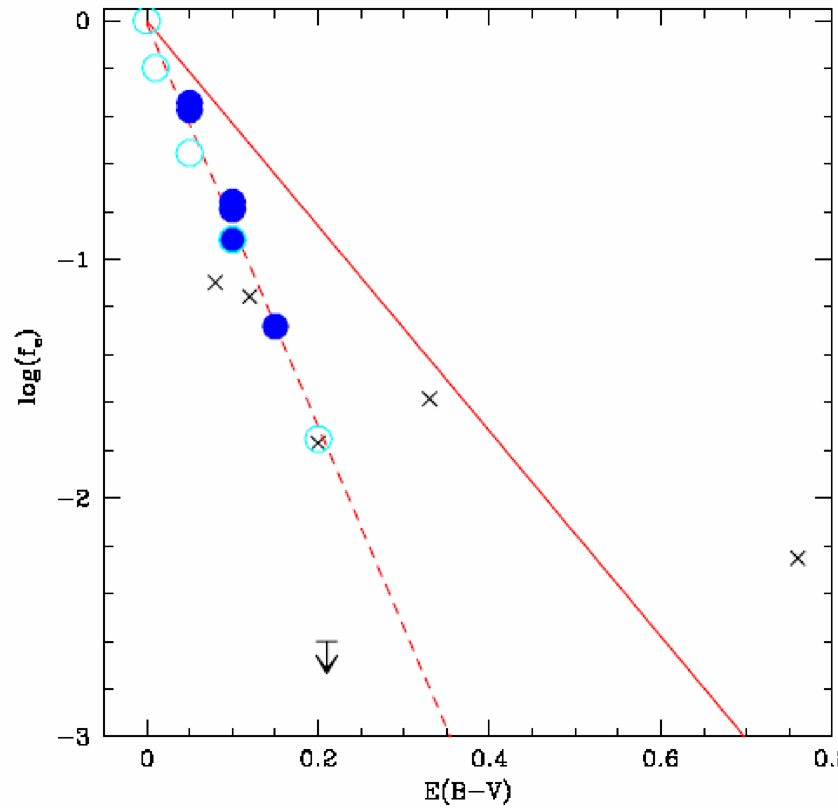

SFR(Lyα) versus SFR(UV)

Better fits

Escape fraction versus extinction

V- Deep surveys

L. Davies
D. Leborgne

Davies, Bremer, Stanway, Lehnert & Douglas

Deep spectro of z>5 objects in the BDF field

VIMOS Ly-α emission line shapes detected from five z ~5 sources in the BDF field, which display line broadening up to and exceeding 600kms^{-1}. ➔ presence of strong galactic winds arising from intense star formation.

Models to explain Ly-α peak velocity offsets from redshift measurements of UV continuum absorption lines in stacked spectra, and the discrepancy between Ly-α and UV continuum derived Star Formation Rate (SFR) estimates.

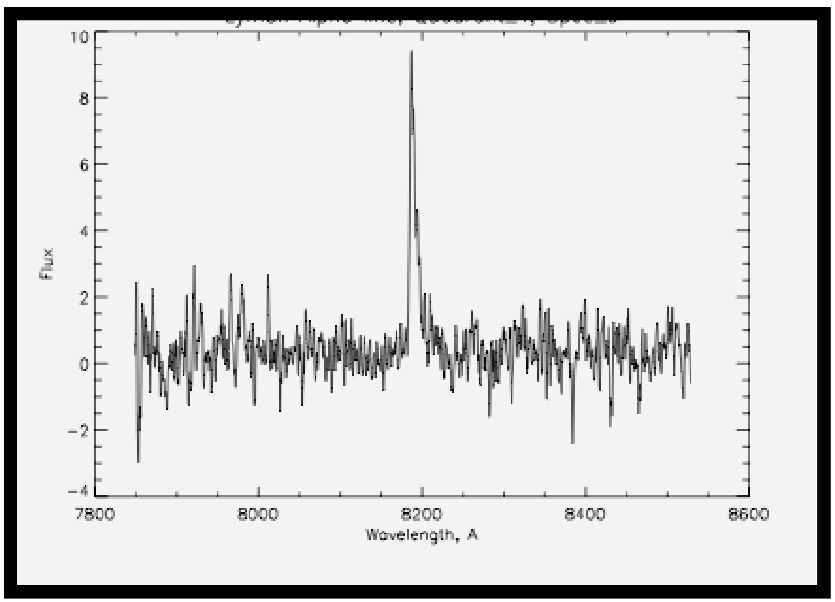

LAE at z=5.6 in BDF

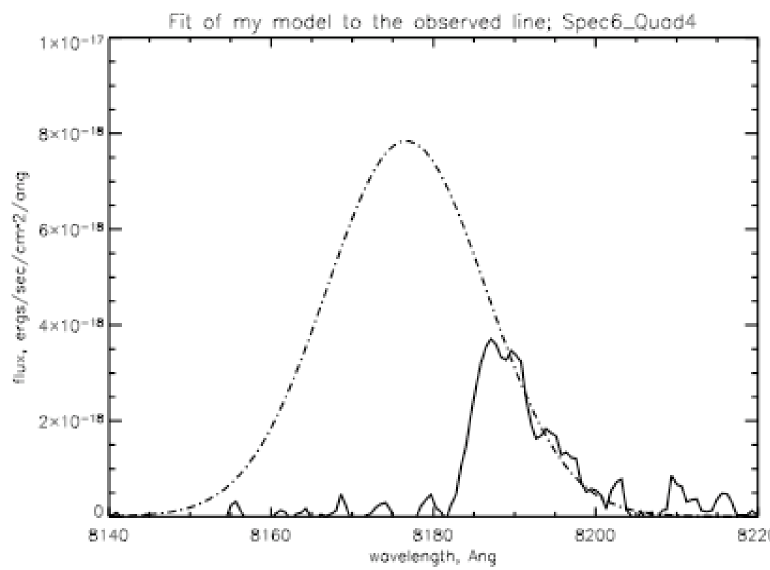

Model of flux through IGM and data

Leborgne, Elbaz, Ocvirk, Pichon

Cosmic SFH from the MIR and FIR up to z ~5

Galaxy counts at
15, 24, 70, 160, 180 μm

→

Non-parametric inversion
(**without any redshift input information** in the general case)

→

Range of possible **evolving total infrared luminosity functions** compatible with current infrared observations

↓

Range of all possible cosmic star-formation histories

Optional prior:
Low-redshift luminosity function measured from 24μm sources

Chary & Elbaz (2001)
library of IR SED templates

Conclusions

1) For the first time, *all the infrared information* available is used *simultaneoulsy* to derive the LF, hence the cosmic star formation history

2) The star-formation activity is better constrained at high redshift